Comparison of Subgenomic and Total RNA in SARS-CoV-2 Challenged Rhesus Macaques

Running Title: Subgenomic RNA in SARS-CoV-2 Challenged Macaques

Gabriel Dagotto[a,b]*, Noe B. Mercado[a]*, David R. Martinez[c], Yixuan J. Hou[c], Joseph P. Nkolola[a], Robert H. Carnahan[d,e], James E. Crowe Jr[d,e,f], Ralph S. Baric[c], and Dan H. Barouch[a,b,g,h,#]

*These authors contributed equally to this work; author order was determined alphabetically.

Corresponding author: D.H.B. (dbarouch@bidmc.harvard.edu)

[a]Center for Virology and Vaccine Research, Beth Israel Deaconess Medical Center, Boston, MA 02215, USA

[b]Harvard Medical School, Boston, MA 02115, USA

[c]Department of Epidemiology, The University of North Carolina at Chapel Hill, Chapel Hill, NC, 27599, USA

[d]Vanderbilt Vaccine Center, Vanderbilt University Medical Center, Nashville, TN, USA.

[e]Department of Pediatrics, Vanderbilt University Medical Center, Nashville, TN, USA.

[f]Department of Pathology, Microbiology, and Immunology, Vanderbilt University Medical Center, Nashville, TN, USA.

[g]Ragon Institute of MGH, MIT, and Harvard, Cambridge, MA 02139, USA

[h]Massachusetts Consortium on Pathogen Readiness, Boston, MA 02215, USA

Abstract Word Count: 215

Manuscript Word Count: 3528

Abstract

Respiratory virus challenge studies involve administration of the challenge virus and sampling to assess for protection from the same anatomical locations. It can therefore be difficult to differentiate actively replicating virus from input challenge virus. For SARS-CoV-2, specific monitoring of actively replicating virus is critical to investigate the protective and therapeutic efficacy of vaccines, monoclonal antibodies, and antiviral drugs. We developed a SARS-CoV-2 subgenomic RNA (sgRNA) RT-PCR assay to differentiate productive infection from inactivated or neutralized virus. Subgenomic RNAs are generated after cell entry and are poorly incorporate into mature virions, and thus may provide a marker for actively replicating virus. We show envelope (E) sgRNA was degraded by RNase in infected cell lysates, while genomic RNA (gRNA) was protected, presumably due to packaging into virions. To investigate the capacity of the sgRNA assay to distinguish input challenge virus from actively replicating virus *in vivo*, we compared the E sgRNA assay to a standard nucleoprotein (N) or E total RNA assay in convalescent rhesus macaques and in antibody-treated rhesus macaques after experimental SARS-CoV-2 challenge. In both studies, the E sgRNA assay was negative, suggesting protective efficacy, whereas the N and E total RNA assays remained positive. These data suggest the potential utility of sgRNA to monitor actively replicating virus in prophylactic and therapeutic SARS-CoV-2 studies.

Importance

Developing therapeutic and prophylactic countermeasures for the SARS-CoV-2 virus is a public health priority. During challenge studies, respiratory viruses are delivered and sampled from the same anatomical location. It is therefore important to distinguish actively replicating

47 virus from input challenge virus. The most common assay for detecting SARS-CoV-2 virus,
48 reverse transcription polymerase chain reaction (RT-PCR) targeting nucleocapsid total RNA,
49 cannot distinguish neutralized input virus from replicating virus. In this study, we assess SARS-
50 CoV-2 subgenomic RNA as a potential measure of replicating virus in rhesus macaques.
51
52

Introduction

Members of the *Coronaviridae* family cause a wide range of respiratory and enteric diseases ranging from mild illness to life threatening infection. This family contains the largest known RNA viral genomes ranging from 26-32 kilobases long(1). Coronaviruses utilize a positive sense, single stranded RNA genome that encodes several nonstructural and structural proteins. Two large polyproteins termed ORF1a and ORF1b encode nonstructural proteins that form the replication-transcription complex(2). The 3' third of the genome consists of the main structural proteins: envelope (E), membrane (M), nucleocapsid (N), and spike (S) as well as other accessory proteins(2). The nonstructural genes are translated upon cytoplasmic entry, but the structural proteins must first be transcribed into subgenomic RNAs (sgRNAs) prior to translation(3). These sgRNA sequences consist of the leader sequence, the transcriptional regulatory sequence (TRS), and the target structural gene followed by the rest of the genome 3' of the gene. Subgenomic transcripts are thought to be generated through a discontinuous transcription model(4, 5). Negative sense sgRNA transcription proceeds 3' to 5' from the 3' end of the genome. Transcription continues until the first TRS preceding each subgenomic gene is reached. At which point a fixed proportion of replication transcription complexes (RTCs) will continue transcription while the rest will stop transcription and transfer to the 5' end of the genome (this is repeated for every subgenomic TRS) to finish transcription adding the leader sequence located at the 5' end of the genome to the subgenomic transcript. This transfer is guided by the complementarity of the TRS sequence on the 3' end of the nascent transcript and the TRS site on proceeding the leader sequence in the 5' end of the genome. Positive sense sgRNA transcripts are then directly transcribed from the negative sense sgRNA transcript(4, 5).In general, the viral sgRNAs are expressed in abundance relative to their proximity to the 3'

end of the genome, such that E sgRNA is much less abundant that N sgRNAs in infected cells(2). Such transcription results in the generation of a set of nested sequences (Fig. 1a)(1, 4).

In December 2019, a novel SARS-like coronavirus emerged(6-8), and SARS-CoV-2 quickly spread throughout the world resulting in a global pandemic(9). Phylogenetic analysis determined SARS-CoV-2 to be a member of the *betacoronavirus* genus containing SARS-CoV(10). Determining the efficacy of candidate vaccines and therapeutics is therefore critical. Quantitating virus genome copy numbers from infected samples has been a reliable way to measure viral load(11, 12). Animal or patient samples are typically reverse transcribed (in the case of RNA viruses) and probed with virus specific primer/probe sets by quantitative polymerase chain reaction (qPCR) to determine viral genome copy numbers(13). This method has also been used in previous outbreak virus vaccine studies such as Zika virus(14). A viral load assay was rapidly developed for SARS-CoV-2 infection monitoring, the most prominent assay detects total RNA containing the N gene(15).

As a respiratory virus, SARS-CoV-2 poses a unique set of challenges concerning vaccine studies. Preclinical studies typically include viral challenges in the respiratory tract, typically by the intranasal and intratracheal routes. Monitoring of infection following challenge uses samples from the same anatomic locations, typically bronchoalveolar lavage, nasal swabs, and respiratory tract tissues(16). An assay targeting total RNA or genomic RNA (gRNA) would presumably detect both input challenge virus as well as newly replicating virus and would not be able to differentiate between them. Thus, monitoring total RNA or gRNA following challenge may not be an optimal measure of protective efficacy.

A potential solution to this problem would be to assess sgRNA instead of gRNA. Subgenomic RNAs are only generated following productive infection and thus should present a

more accurate measure of replicating virus. A sgRNA assay was originally described by Wölfel *et al.* (2020) (17), and we developed this assay for use in SARS-CoV-2 challenge studies in rhesus macaques(16). This assay has also recently been used by other groups conducting vaccine/challenge studies in rhesus macaques(18-20) making it critical to understand how subgenomic RNA differs from total RNA in the model. In this paper, we demonstrate the importance of targeting subgenomic RNA to differentiate productive infection from neutralized input virus in treated rhesus macaques.

Results

E sgRNA Specificity

After SARS-CoV-2 enters cells, a nested series of sgRNAs are generated(1, 4). The sgRNA RT-PCR assay was designed to target E sgRNA. We utilized a forward primer targeting the subgenomic leader sequence and a reverse primer and probe specific to the E gene(17).These primers span the junction between the subgenomic leader sequence and the E gene providing high selectivity for E sgRNA (Fig 1b). To demonstrate the specificity of this assay, qPCR products from SARS-CoV-2 infected macaques were run on an agarose gel (Fig 2). The resulting gel had a single band for all positive samples at the expected size for the target amplicon (179 bp). Positive macaque qPCR amplicons were the same size as the E sgRNA positive control further confirming assay specificity. The bands were sequenced and found to match the expected target amplicon.

In order to confirm the E sgRNA primer/probe set targets only E sgRNA, we designed DNA fragments of multiple SARS-CoV-2 structural and non-structural genes. Mixtures of DNA fragments with and without DNA corresponding to E sgRNA were evaluated by qPCR using the E sgRNA primer/probe set. Three different mixtures were generated testing E sgRNA specificity against the full length (Fig 3a) and subgenomic structural genes (Fig 3b) as well as gRNA which contains a 5' subgenomic leader sequence (Fig 3c). Specific amplification over a 6-log dilution range was only observed in the presence of DNA corresponding to E sgRNA. As a control, qPCR assays for E gRNA amplified both mixtures (Fig 3 d,e).

Lack of RNA amplification in virions by sgRNA assay

The E sgRNA assay should only amplify transcripts in the setting of active virus replication that produces sgRNA and should not amplify genomic RNA (gRNA). Laboratory virus stocks are typically cell lysates, which contain predominantly gRNA but also sgRNA from virus replication in cells. We therefore treated cell lysates with RNase A to degrade unpackaged RNA, but capsid-packaged gRNA should be protected.

We extracted RNA from the RNase A treated infection lysate and performed RT-PCR for the N total RNA (both gRNA and sgRNA), E sgRNA, and the Orf1ab gene that includes only gRNA, since Orf1ab does not generate subgenomic transcripts(21). After RNase A treatment, the median E sgRNA signal was at the limit of detection. Median Orf1ab and N total viral loads were $>10^4$ and $>10^5$ RNA copies per µg RNA, respectively (Fig 4). The difference in N total and Orf1ab could be due to insufficient RNase A levels or trace amounts of N sgRNA packaged into virions(22). These data demonstrate that the E sgRNA assay does not detect genomic SARS-CoV-2 RNA in RNase-treated virions.

Measuring sgRNA and gRNA during infection *in vitro*

We next monitored E sgRNA, N total RNA, and Orf1ab gRNA longitudinally following SARS-CoV-2 infection in Vero-E6 cells. Cells were infected at an MOI of 0.1 or 1.0 in a 12-well plates. At 0, 2, 4, 6, 8, 12, and 24 hours post infection RNA was extracted for RT-PCR. At 2 h following infection, substantially lower levels of E sgRNA were observed compared with N total RNA or Orf1ab gRNA (Fig 5), likely reflecting the different molar ratios of sgRNA produced within cells(2, 23). From 2-8 hours post infection, all three RNA measurements showed comparable growth as expected(4, 24). Interestingly, after 12 hours gRNA appeared to increase

at a faster rate than sgRNA, particularly with the 1.0 MOI inoculation, likely reflecting the typically higher levels of gRNA compared with sgRNA in infected cells.

Monitoring sgRNA and total RNA in NHP SARS-CoV-2 challenge studies

We hypothesized that the E sgRNA assay would be useful for monitoring viral loads in SARS-CoV-2 challenge studies in nonhuman primates (NHPs), as it should be able to distinguish input challenge virus from newly replicating virus. We have recently reported a study of SARS-CoV-2 infection in rhesus macaques and protection against re-challenge(16). Rhesus macaques were infected with 10^5 $TCID_{50}$ SARS-CoV-2 virus intranasally and intratracheally and were re-challenged with 10^5 $TCID_{50}$ on day 35(16). Following re-challenge, there was a median of $>10^3$ N total RNA copies/ml in these animals on day 1 that declined by day 3, but undetectable E sgRNA copies/ml (Fig 6). These data suggest that the N total RNA likely reflected input challenge virus, and that the amount of active virus replication following re-challenge was below the detection limit. In contrast, both N total RNA and E sgRNA were robustly detected in animals by day 2 following primary infection of naïve animals (Fig 6).

Finally, we evaluated viral loads from macaques that received the monoclonal SARS-CoV-2 antibodies COV2-2196 and COV2-2381. We have recently reported that rhesus macaques that received 50 mg/kg intravenously of these SARS-CoV-2 mAbs were protected against challenge with 10^5 $TCID_{50}$ SARS-CoV-2 (25). Low levels of N total and E total RNA was nevertheless detectable on days 1-2 following challenge, likely reflecting input challenge virus, whereas E sgRNA was negative at all timepoints (Fig 7). The direct comparison of E total RNA and E sgRNA excludes the possibility that the E gene is simply less sensitive than the N gene, given that prior experiments used only N for measuring total RNA.

Subgenomic RT-PCR viral assay qualification for human use

Lastly, we qualified the SARS-CoV-2 E sgRNA RT-PCR assay for inter and intra precision, assay range, and limit of detection (LOD) using SARS-CoV-2 positive human nasopharyngeal swabs. Tandem assay precision and dilutional linearity were performed to establish the upper limit of quantification (ULOQ) with percent relative standard deviation (%RSD) ≤25%. Resulting in a ULOQ of 6.57 log RNA copies/ml. LOD determination was based on two-fold serial dilutions of positive human nasopharyngeal swabs (Table 1). The 95% confidence interval was determined for the lowest detectable RNA copies in the sample dilutions and the LOD defined as the lower limit of this confidence interval resulting in a LOD value of 2.71 log RNA copies/ml. The assay range was thus determined to have a range of 2.71-6.57 log RNA copies/ml. The mean intermediate precision %RSD within this assay range was 4.7% (Table 2). Intra-assay precision within the linear range was established with a pre-defined ≤25% %RSD and gave an overall precision of 1.85% (Table 3).

Discussion

It is critical for SARS-CoV-2 vaccine and therapeutic studies in rhesus macaques to differentiate input challenge virus from actively replicating virus. Our data demonstrate the potential of measuring sgRNA rather than genomic or total RNA as a more specific measure of replicating virus (4, 16, 18, 24).

SARS-CoV-2 challenge studies administer virus and then sample from the same anatomic sites to assess protective efficacy. RT-PCR assays typically target total RNA, which is present in the input challenge virus. Therefore, an assay that amplifies gRNA (or total RNA)

would not be expected to differentiate input or neutralized virus from newly replicating virus. This would make distinguishing vaccine or drug effects difficult at early time points. In contrast, sgRNAs are generated after cell entry in the context of active viral replication. Measuring sgRNA presents a more accurate RT-PCR assay for monitoring the impact of vaccines, mAbs, or other interventions on SARS-CoV-2 virus replication**.** This E sgRNA assay allowed us to differentiate input and replicating virus for assessing the protective efficacy of natural immunity or mAbs in NHP models (16, 25).

The subgenomic E (sgE) gene was used to measure sgRNA levels in this work(17). In the future, it may be reasonable to explore other sgRNAs in similar assays to increase sensitivity. In particular, the sgE gene is transcribed at a lower level than the subgenomic N gene(2, 21). In summary, total RNA or gRNA may not be an optimal measure of protective efficacy following SARS-CoV-2 challenge, as it includes input challenge virus, and sgRNA may be more relevant for measuring actively replicating virus in vivo. These findings are important for the evaluation of SARS-CoV-2 prophylactic and therapeutic agents.

Materials and Methods

Synthetic genes: Genomic and subgenomic genes were synthesized based on the SARS-CoV-2 USA-WA1/2020 (GenBank: MN985325.1) and following the schematic previously described(17). All subgenomic genes contain the SARS-CoV-2 leader sequence followed by the TRS (ATGG) and the structural gene Spike (S), Envelope (E), Membrane (M), Nucleocapsid (N). Genes were synthesized by Integrated DNA Technologies and confirmed by sequencing. Standard curves were generated for each synthetic gene by cloning into a pcDNA3.1 expression plasmid then *in vitro* transcribing using an AmpliCap-Max T7 High Yield Message Maker Kit (Cellscript). Log dilutions of the resulting *in vitro* transcribed RNA were prepared.

RT-PCR: The RNA transcripts were reverse transcribed using Superscript III VILO (Invitrogen) according to the manufacturer's instructions. A Taqman custom gene expression assay (ThermoFisher Scientific) was designed to specifically target each genomic and subgenomic synthetic gene. The samples were run in duplicate QuantStudio 6 Flex Real-Time PCR System (Life Technologies) using the following conditions: 95℃ for 20 seconds then 45 cycles of 95℃ for 1 second and 60℃ for 20 seconds. For all RT-PCR runs the following QC acceptance range for standard curves must be met $R2 > 0.98$, Efficiency 90-110%, and Slope $-3.1 < x > -3.6$. The amplified RT-PCR products were run on 0.8% agarose gel for confirmation of subgenomic E amplification.

Primer sequences (Table 4): RT-PCR was performed on the E subgenomic gene using the leader forward primer; sgLeadCoV2.Fwd: CGATCTCTTGTAGATCTGTTCTC, and the complementing probes and reverse primers as follows:

Journal of Virology

E sgRNA: E_Sarbeco_R: ATATTGCAGCAGTACGCACACA, E_Sarbeco_P1 (probe): VIC-ACACTAGCCATCCTTACTGCGCTTCG-MGB. RT-PCR was also performed on the ORF1ab gene using the following, CoV2.ORF1ab.F: GGCCAATTCTGCTGTCAAATTA, CoV2.ORF1ab.R: CAGTGCAAGCAGTTTGTGTAG, CoV2.ORF1ab.P: FAM-ACAGATGTCTTGTGCTGCCGGTA-BHQ. The complementing N total structural gene primers and probe were used as describe previously(15).

RNase A treated SARS-CoV-2 *in vitro* infection: SARS-CoV-2 virus stocks were diluted to a 0.1 and 1.0 MOI in infection media and treated with 200 µl or 20 µl of RNase A (Sigma: R4642) for 1 hour at 37°C. Infection media negative control was also treated with 200 µl or 20 µl of RNase A for 1 hour at 37°C. SARS-CoV-2 treated stocks were then lysed with 500 µl of TRizol Reagent. Total RNA was extracted from cells using a QIAcube HT (Qiagen) and RNeasy 96 QIAcube HT Kit (Qiagen). RNA was reverse transcribed into cDNA using superscript VILO (Invitrogen). RT-PCR was performed as described above.

***In vitro* SARS-CoV-2 infection:** Vero-E6 cells were seeded in 12-well plates (Corning) at 300,000 cells per well the day prior to infection in growth media (DMEM, 5% Fetal Clone II, 1% antibiotic-antimycotic). On the day of infection, SARS-CoV-2 infectious viral particles were treated with 25 units of RNase H (Promega: M4281) for 1 hour at 37°C. Cells were then infected in triplicate wells at a 0.1 or 1.0 multiplicity of infection (MOI) of RNase H-treated SARS-CoV-2 and RNase H-treated infection media (DMEM, 2% Fetal Clone II, 1% antibiotic-antimycotic) negative control for 1 hour at 37°C. Following infection, Vero-E6 cells were thoroughly washed three times with 1ml of sterile 1X PBS and 500 µl of infection media was replaced in each well.

Cells were then harvested at 2, 4, 6, 8, 12, and 24 hours post infection. Prior to harvesting each timepoint, cells were twice washed with 1 ml of sterile 1X PBS, lysed with 300 µl of TRIzol Reagent, and were immediately frozen. Total RNA was extracted from cells using a QIAcube HT (Qiagen) and RNeasy 96 QIAcube HT Kit (Qiagen). RNA was reverse transcribed into cDNA using superscript VILO (Invitrogen). RT-PCR was performed as described above.

NHP monoclonal antibody studies: As part of the study 12 healthy female and male rhesus macaques (*Macaca mulatta*) of Indian origin ranging in weight from 5 to 15 kg were studied as previously described(25). The monkeys were randomly allocated into three groups, group 1; anti-SARS CoV-2 mAb COV2-2196 (N=4), group 2; anti-SARS CoV-2 mAb COV2-2381 (N=4), group 3; sham IgG (N=4). The animals were given one dose 50 mg/kg of anti-SARS-CoV-2 antibody or sham isotype intravenously on day -3. All animals were subsequently challenged with 10^5 $TCID_{50}$ SARS-CoV-2, administered as 1 ml by the intranasal route and 1 ml by the intratracheal route on day 3 post antibody infusion. All animal studies were conducted in compliance with all relevant local, state, and federal regulations and were approved by the Bioqual Institutional Animal Care and Use Committee (IACUC).

Viral RNA was quantified using an RT-PCR assay targeting the SARS-CoV-2 nucleocapsid and subgenomic envelope genes. RNA was isolated from nasal swabs and BAL collected from macaques using the cador Pathogen 96 QIAcube HT Kit and a Qiacube HT (QIAGEN). RT-PCR was performed as described above.

NHP re-challenge model: Three outbred Indian-origin adult male and female rhesus macaques (*Macaca mulatta*), 6-12 years old, were used to set up the RT-PCR assays, which were previously reported(16). All animals were housed at Bioqual, Inc. (Rockville, MD). All animals were inoculated with SARS-CoV-2 at a total dose of 10^5 $TCID_{50}$ on day 0. The dose was administered as 1 ml by the intranasal (IN) route (0.5 ml in each nare) and 1 ml by the intratracheal (IT) route. On day 35 following challenge, animals were re-challenged with SARS-CoV-2 with the same dose utilized in the initial challenge. All animal studies were conducted in compliance with all relevant local, state, and federal regulations and were approved by the Bioqual Institutional Animal Care and Use Committee (IACUC). RT-PCR was performed as described above.

Subgenomic assay qualification: Reverse transcribed cDNA (derived from pooled RNA extracted from the nasopharyngeal swab samples of SARS-CoV-2 infected individuals with viral $>10^7$ copies/mL was tested undiluted and serially diluted (in log dilutions) to assess linearity and intermediate precision for the subgenomic viral RNA assay. Three different operators performed these assays over three different days for each assay run. The highest value of the sample dilution range with a precision of relative standard deviation (RSD) ≤25% was used to define the Upper Limit of Quantification (ULOQ). To determine intra-assay precision, two cDNA dilutions within the linear range were selected to approximate high and low levels of the ranges. At these approximate high and low levels, pre-defined intra-assay precision of RSD ≤25% was met by each individual operator.

Limit of detection: Serial dilutions of ten individual SARS-CoV-2 positive cDNA samples from nasopharyngeal swabs derived from positive individuals were tested in two-fold dilutions.

Within each dilution series, the last positive value or last positive value prior to sample becoming undetectable was used in LOD calculations. Any positive values observed beyond the first undetectable result in a dilution series were considered not valid. The 95% confidence interval was obtained for these samples and the LOD defined as the lower limit of this confidence interval reported as log RNA copies/ml.

Author contributions: G.D., N.B.M., and D.H.B. designed the study and reviewed all data. D.R.M., Y.J.H., and R.S.B performed the *in vitro* longitudinal infections. J.P.N. performed assay qualification. G.D. and N.B.M. performed virologic assays. R.H.C., J.E.C., and D.H.B. performed the monoclonal antibody experiment. G.D., N.B.M., and D.H.B wrote the paper with all co-authors.

Acknowledgements: We thank Z. Lin, A. Collier, F. Nampanya, S. Patel, C. Jacob-Dolan, and M. Gebre for generous advice, assistance, and reagents.

Funding: We acknowledge support from the Ragon Institute of MGH, MIT, and Harvard, Massachusetts Consortium on Pathogen Readiness (MassCPR), and the National Institutes of Health (AI124377, AI128751, AI126603, AI142759, AI152296, CA260476). David R. Martinez is also funded by a Burroughs Wellcome Fund Postdoctoral Enrichment Program Award.

References

1. Fehr AR, Perlman S. 2015. Coronaviruses: An Overview of Their Replication and Pathogenesis, p 1-23. *In* Maier HJ, Bickerton E, Britton P (ed), Coronaviruses: Methods and Protocols doi:10.1007/978-1-4939-2438-7_1. Springer New York, New York, NY.
2. Hou YJ, Okuda K, Edwards CE, Martinez DR, Asakura T, Dinnon KH, Kato T, Lee RE, Yount BL, Mascenik TM, Chen G, Olivier KN, Ghio A, Tse LV, Leist SR, Gralinski LE, Schäfer A, Dang H, Gilmore R, Nakano S, Sun L, Fulcher ML, Livraghi-Butrico A, Nicely NI, Cameron M, Cameron C, Kelvin DJ, de Silva A, Margolis DM, Markmann A, Bartelt L, Zumwalt R, Martinez FJ, Salvatore SP, Borczuk A, Tata PR, Sontake V, Kimple A, Jaspers I, O'Neal WK, Randell SH, Boucher RC, Baric RS. 2020. SARS-CoV-2 Reverse Genetics Reveals a Variable Infection Gradient in the Respiratory Tract. Cell 182:429-446.e14.
3. Song Z, Xu Y, Bao L, Zhang L, Yu P, Qu Y, Zhu H, Zhao W, Han Y, Qin C. 2019. From SARS to MERS, thrusting coronaviruses into the spotlight. Viruses 11:59.
4. Sawicki SG, Sawicki DL, Siddell SG. 2007. A Contemporary View of Coronavirus Transcription. Journal of Virology 81:20-29.
5. Sola I, Almazán F, Zúñiga S, Enjuanes L. 2015. Continuous and Discontinuous RNA Synthesis in Coronaviruses. Annual Review of Virology 2:265-288.
6. Chan JF-W, Yuan S, Kok K-H, To KK-W, Chu H, Yang J, Xing F, Liu J, Yip CC-Y, Poon RW-S, Tsoi H-W, Lo SK-F, Chan K-H, Poon VK-M, Chan W-M, Ip JD, Cai J-P, Cheng VC-C, Chen H, Hui CK-M, Yuen K-Y. 2020. A familial cluster of pneumonia associated with the 2019 novel coronavirus indicating person-to-person transmission: a study of a family cluster. The Lancet 395:514-523.
7. Li Q, Guan X, Wu P, Wang X, Zhou L, Tong Y, Ren R, Leung KSM, Lau EHY, Wong JY, Xing X, Xiang N, Wu Y, Li C, Chen Q, Li D, Liu T, Zhao J, Liu M, Tu W, Chen C, Jin L, Yang R, Wang Q, Zhou S, Wang R, Liu H, Luo Y, Liu Y, Shao G, Li H, Tao Z, Yang Y, Deng Z, Liu B, Ma Z, Zhang Y, Shi G, Lam TTY, Wu JT, Gao GF, Cowling BJ, Yang B, Leung GM, Feng Z. 2020. Early Transmission Dynamics in Wuhan, China, of Novel Coronavirus–Infected Pneumonia. New England Journal of Medicine 382:1199-1207.
8. Yu J, Tostanoski LH, Peter L, Mercado NB, McMahan K, Mahrokhian SH, Nkolola JP, Liu J, Li Z, Chandrashekar A, Martinez DR, Loos C, Atyeo C, Fischinger S, Burke JS, Slein MD, Chen Y, Zuiani A, N. Lelis FJ, Travers M, Habibi S, Pessaint L, Van Ry A, Blade K, Brown R, Cook A, Finneyfrock B, Dodson A, Teow E, Velasco J, Zahn R, Wegmann F, Bondzie EA, Dagotto G, Gebre MS, He X, Jacob-Dolan C, Kirilova M, Kordana N, Lin Z, Maxfield LF, Nampanya F, Nityanandam R, Ventura JD, Wan H, Cai Y, Chen B, Schmidt AG, Wesemann DR, Baric RS, et al. 2020. DNA vaccine protection against SARS-CoV-2 in rhesus macaques. Science doi:10.1126/science.abc6284:eabc6284.
9. WHO. 2020. WHO Director-General's opening remarks at the media briefing on COVID-19 - 11 March 2020. https://www.who.int/dg/speeches/detail/who-director-general-s-opening-remarks-at-the-media-briefing-on-covid-19---11-march-2020. Accessed
10. Lu R, Zhao X, Li J, Niu P, Yang B, Wu H, Wang W, Song H, Huang B, Zhu N, Bi Y, Ma X, Zhan F, Wang L, Hu T, Zhou H, Hu Z, Zhou W, Zhao L, Chen J, Meng Y, Wang J, Lin Y, Yuan J, Xie Z, Ma J, Liu WJ, Wang D, Xu W, Holmes EC, Gao GF, Wu G, Chen W, Shi W, Tan W. 2020. Genomic characterisation and epidemiology of 2019 novel coronavirus: implications for virus origins and receptor binding. The Lancet 395:565-574.
11. Santiago GA, Vergne E, Quiles Y, Cosme J, Vazquez J, Medina JF, Medina F, Colón C, Margolis H, Muñoz-Jordán JL. 2013. Analytical and Clinical Performance of the CDC Real Time RT-PCR Assay for Detection and Typing of Dengue Virus. PLOS Neglected Tropical Diseases 7:e2311.

12. Faye O, Faye O, Dupressoir A, Weidmann M, Ndiaye M, Alpha Sall A. 2008. One-step RT-PCR for detection of Zika virus. Journal of Clinical Virology 43:96-101.
13. Kralik P, Ricchi M. 2017. A Basic Guide to Real Time PCR in Microbial Diagnostics: Definitions, Parameters, and Everything. Frontiers in Microbiology 8.
14. Larocca RA, Abbink P, Peron JPS, de A. Zanotto PM, Iampietro MJ, Badamchi-Zadeh A, Boyd M, Ng'ang'a D, Kirilova M, Nityanandam R, Mercado NB, Li Z, Moseley ET, Bricault CA, Borducchi EN, Giglio PB, Jetton D, Neubauer G, Nkolola JP, Maxfield LF, De La Barrera RA, Jarman RG, Eckels KH, Michael NL, Thomas SJ, Barouch DH. 2016. Vaccine protection against Zika virus from Brazil. Nature 536:474-478.
15. CDC. 2020. Interim Guidelines for Collecting, Handling, and Testing Clinical Specimens for COVID-19. https://www.cdc.gov/coronavirus/2019-nCoV/lab/guidelines-clinical-specimens.html. Accessed
16. Chandrashekar A, Liu J, Martinot AJ, McMahan K, Mercado NB, Peter L, Tostanoski LH, Yu J, Maliga Z, Nekorchuk M, Busman-Sahay K, Terry M, Wrijil LM, Ducat S, Martinez DR, Atyeo C, Fischinger S, Burke JS, Slein MD, Pessaint L, Van Ry A, Greenhouse J, Taylor T, Blade K, Cook A, Finneyfrock B, Brown R, Teow E, Velasco J, Zahn R, Wegmann F, Abbink P, Bondzie EA, Dagotto G, Gebre MS, He X, Jacob-Dolan C, Kordana N, Li Z, Lifton MA, Mahrokhian SH, Maxfield LF, Nityanandam R, Nkolola JP, Schmidt AG, Miller AD, Baric RS, Alter G, Sorger PK, Estes JD, et al. 2020. SARS-CoV-2 infection protects against rechallenge in rhesus macaques. Science doi:10.1126/science.abc4776:eabc4776.
17. Wölfel R, Corman VM, Guggemos W, Seilmaier M, Zange S, Müller MA, Niemeyer D, Jones TC, Vollmar P, Rothe C, Hoelscher M, Bleicker T, Brünink S, Schneider J, Ehmann R, Zwirglmaier K, Drosten C, Wendtner C. 2020. Virological assessment of hospitalized patients with COVID-2019. Nature 581:465-469.
18. Mercado NB, Zahn R, Wegmann F, Loos C, Chandrashekar A, Yu J, Liu J, Peter L, McMahan K, Tostanoski LH, He X, Martinez DR, Rutten L, Bos R, van Manen D, Vellinga J, Custers J, Langedijk JP, Kwaks T, Bakkers MJG, Zuijdgeest D, Huber SKR, Atyeo C, Fischinger S, Burke JS, Feldman J, Hauser BM, Caradonna TM, Bondzie EA, Dagotto G, Gebre MS, Hoffman E, Jacob-Dolan C, Kirilova M, Li Z, Lin Z, Mahrokhian SH, Maxfield LF, Nampanya F, Nityanandam R, Nkolola JP, Patel S, Ventura JD, Verrington K, Wan H, Pessaint L, Ry AV, Blade K, Strasbaugh A, Cabus M, et al. 2020. Single-shot Ad26 vaccine protects against SARS-CoV-2 in rhesus macaques. Nature doi:10.1038/s41586-020-2607-z.
19. van Doremalen N, Lambe T, Spencer A, Belij-Rammerstorfer S, Purushotham JN, Port JR, Avanzato VA, Bushmaker T, Flaxman A, Ulaszewska M, Feldmann F, Allen ER, Sharpe H, Schulz J, Holbrook M, Okumura A, Meade-White K, Pérez-Pérez L, Edwards NJ, Wright D, Bissett C, Gilbride C, Williamson BN, Rosenke R, Long D, Ishwarbhai A, Kailath R, Rose L, Morris S, Powers C, Lovaglio J, Hanley PW, Scott D, Saturday G, de Wit E, Gilbert SC, Munster VJ. 2020. ChAdOx1 nCoV-19 vaccine prevents SARS-CoV-2 pneumonia in rhesus macaques. Nature doi:10.1038/s41586-020-2608-y.
20. Corbett KS, Flynn B, Foulds KE, Francica JR, Boyoglu-Barnum S, Werner AP, Flach B, O'Connell S, Bock KW, Minai M, Nagata BM, Andersen H, Martinez DR, Noe AT, Douek N, Donaldson MM, Nji NN, Alvarado GS, Edwards DK, Flebbe DR, Lamb E, Doria-Rose NA, Lin BC, Louder MK, O'Dell S, Schmidt SD, Phung E, Chang LA, Yap C, Todd J-PM, Pessaint L, Van Ry A, Browne S, Greenhouse J, Putman-Taylor T, Strasbaugh A, Campbell T-A, Cook A, Dodson A, Steingrebe K, Shi W, Zhang Y, Abiona OM, Wang L, Pegu A, Yang ES, Leung K, Zhou T, Teng I-T, Widge A, et al. 2020. Evaluation of the mRNA-1273 Vaccine against SARS-CoV-2 in Nonhuman Primates. New England Journal of Medicine doi:10.1056/NEJMoa2024671.

21. Kim D, Lee J-Y, Yang J-S, Kim JW, Kim VN, Chang H. 2020. The architecture of SARS-CoV-2 transcriptome. Cell.
22. Makino S, Shieh C-K, Keck JG, Lai MMC. 1988. Defective-interfering particles of murine coronavirus: Mechanism of synthesis of defective viral RNAs. Virology 163:104-111.
23. Sethna PB, Hung S-L, Brian DA. 1989. Coronavirus subgenomic minus-strand RNAs and the potential for mRNA replicons. Proceedings of the National Academy of Sciences 86:5626-5630.
24. Sawicki S, Sawicki D. 2005. Coronavirus transcription: a perspective, p 31-55, Coronavirus replication and reverse genetics. Springer.
25. Zost SJ, Gilchuk P, Case JB, Binshtein E, Chen RE, Nkolola JP, Schäfer A, Reidy JX, Trivette A, Nargi RS, Sutton RE, Suryadevara N, Martinez DR, Williamson LE, Chen EC, Jones T, Day S, Myers L, Hassan AO, Kafai NM, Winkler ES, Fox JM, Shrihari S, Mueller BK, Meiler J, Chandrashekar A, Mercado NB, Steinhardt JJ, Ren K, Loo Y-M, Kallewaard NL, McCune BT, Keeler SP, Holtzman MJ, Barouch DH, Gralinski LE, Baric RS, Thackray LB, Diamond MS, Carnahan RH, Crowe JE. 2020. Potently neutralizing and protective human antibodies against SARS-CoV-2. Nature doi:10.1038/s41586-020-2548-6.

435 **Figure Legends**

436

437 **Figure 1: Graphical representation of sgRNAs and the E sgRNA assay.** (a) Graphical
438 representation of SARS-COV-2 virus and sgRNA. Upon cellular entry SARS-CoV-2 generates
439 sgRNAs for structural genes and accessory proteins before they are produced. The subgenomic
440 leader sequence is colored cyan to highlight its position in the genomic and subgenomic RNAs.
441 (b) Graphical representation of the primer binding sites for the E sgRNA assay on subgenomic E
442 RNA. The forward primer binds to the subgenomic leader sequence present on all subgenomic
443 RNAs as well as the genomic RNA. The reverse primer binds to the E gene (pink).

444

445 **Figure 2:** SARS-CoV-2 infected NHPs were sampled through nasal swabs on D4 post infection.
446 (a) RNA was extracted from the nasal swabs and E sgRNA RT-PCR assay was performed. (b)
447 The assay RT-PCR results were then run in duplicate on a 0.8% agarose gel to confirm a single
448 amplicon. Error bars define the standard deviation of the mean of two technical replicates for
449 each macaque.

450

451 **Figure 3: Assay specificity with DNA mixtures.** RT-PCR was performed on DNA fragment
452 mixtures with and without the addition of E sgRNA linear DNA fragments. These mixtures were
453 serially diluted 10-fold from 10^8 to 10 copies per ml. (a) Mixture of E, M, N, and S full length
454 DNA fragments (b) mixture of M, N, and S subgenomic DNA fragments (c) mixture of E and M
455 full length DNA fragments, and the 5' end of Orf1a containing the subgenomic leader sequence.
456 In all mixtures, linearity was only present after the addition of E sgRNA. RT-PCR targeting E
457 gRNA was performed on DNA fragment mixtures with and without the addition of a E sgRNA

DNA fragment. (d) Mixture of E, M, N, and S full length DNA fragments (e) mixture of M, N, and S subgenomic DNA fragments. Error bars describe the 95% confidence intervals of the mean of eight technical replicates. Lines represent simple linear regressions.

Figure 4: Infectious cell lysate treated with RNase A. Infectious cell lysate was treated with RNase A for 1 hour then RNA was extracted and RT-PCR for the N gene (N total), subgenomic E (E sgRNA), and genomic RNA (Orf1ab) was performed. Black bars represent median responses.

Figure 5: Longitudinal SARS-CoV-2 infection. Vero-E6 cells were infected at (a) 0.1 MOI or (b) 1.0 MOI in 12 well plates. Wells were harvested in triplicate at the following timepoints: 0, 2, 4, 6, 8, 12, and 24 hours post infection. Log RNA copies were reported per gram of total RNA.

Figure 6: Convalescent NHP SARS-CoV-2 RT-PCR. NHPs were challenged with SARS-CoV-2 and re-challenged 35 days later. RNA extracted from nasal swabs from the re-challenge macaques was run for N total and E sgRNA in naïve and the same convalescent animals.

Figure 7: Monoclonal antibody protected NHP SARS-CoV-2 RT-PCR. NHPs were given 50 mg/kg of a monoclonal SARS-CoV-2 antibody then challenged three days later with SARS-CoV-2. RNA extracted by BAL was measured for N total, E total, and E sgRNA. Protected macaques (mAb) were compared to unprotected macaques (sham) to demonstrate assay success.

Table 1: Tandem dilutional linearity and intermediate precision for subgenomic viral RNA RT-PCR assay (geomean = geometric mean, Std Dev = standard deviation, RSD = relative standard deviation, * = undetermined).

Subgenomic Viral RNA		Log RNA copies/mL									
		1	**2**	**3**	**4**	**5**	**6**	**7**	**8**	**9**	**10**
cDNA Dilution	**Undiluted**	4.18	5.12	3.81	*	4.14	3.60	5.23	*	3.68	5.48
	1:1	3.94	4.93	3.65	*	3.85	2.98	4.98	*	3.67	5.19
	1:2	3.57	4.53	3.16	*	3.03	3.54	4.63	*	3.15	4.58
	1:4	3.08	4.23	2.80	*	2.71	*	4.36	*	3.12	4.24
	1:8	*	3.81	2.57	*	*	*	4.01	*	2.75	3.89
	1:16	*	3.42	*	*	2.94	*	3.67	*	*	3.72
	1:32	*	3.00	*	*	*	*	3.21	*	*	3.41
	1:64	*	3.34	2.52	*	2.83	*	2.83	*	2.12	2.41
	1:128	*	*	*	*	*	*	3.27	*	*	2.90
	1:256	*	*	*	*	*	*	2.85	*	*	2.63
	1:512	*	2.26	*	*	*	*	2.93	*	*	*
	1:1024	*	*	*	*	*	*	*	*	*	*

Table 2: Established parameters for the subgenomic viral RT-PCR assay (RSD = relative standard deviation).

Parameter	Subgenomic RNA
Assay Range (log RNA copies/ml)	3.24 – 6.57
Intermediate Precision (%RSD)	4.77%
Intra-Assay Precision (%RSD)	1.85%
Limit of Detection (log RNA copies/ml)	2.71

Table 3: Intra-assay precision for total viral RNA RT-PCR assay (geomean = geometric mean, Std Dev = standard deviation, RSD = relative standard deviation)

Subgenomic Viral RNA		**Operator 1**						
		Log RNA copies/mL			**GeoMean**	**Std Dev**	**%RSD**	**Pass/Fail**
		Run 1	**Run 2**	**Run 3**				
cDNA Dilution	**1:10**	5.66	5.50	5.44	5.53	0.11	2.02	Pass
	1:1000	3.63	3.56	3.63	3.61	0.04	1.07	Pass
Subgenomic Viral RNA		**Operator 2**						
		Log RNA copies/mL			**GeoMean**	**Std Dev**	**%RSD**	**Pass/Fail**

		Run 1	Run 2	Run 3				
cDNA Dilution	**1:10**	5.52	5.53	5.66	5.57	0.07	1.32	Pass
	1:1000	3.77	3.49	3.80	3.68	0.17	4.70	Pass
Subgenomic Viral RNA		**Operator 3**						
		Log RNA copies/mL			**GeoMean**	**Std Dev**	**%RSD**	**Pass/Fail**
		Run 1	**Run 2**	**Run 3**				
cDNA Dilution	**1:10**	5.36	5.41	5.33	5.36	0.04	0.75	Pass
	1:1000	3.38	3.44	3.36	3.39	0.04	1.27	Pass

Table 4: Primers and probes for RT-PCR.

Gene	Oligonucleotide	Primer/probe	Sequence 5' to 3'	Concentration
Subgenomic Envelope (E)	sgLeadCoV2.Fwd	Forward Primer	CGATCTCTTGTAGATCTGTTCTC	20uM
Envelope (E)	E_Sarbeco_F	Forward Primer	ACAGGTACGTTAATAGTTAATAGCGT	20uM
	E_Sarbeco_R	Reverse Primer	ACAGGTACGTTAATAGTTAATAGCGT	20uM
	E_Sarbeco_P1	Probe	FAM-ACACTAGCCATCCTTACTGCGCTTCG-BBQ	10nmol
Nucleocapsid	2019-nCoV_N1-F	Forward Primer	GAC CCC AAA ATC AGC GAA AT	20uM

(N)				
	2019-nCoV_N1-R	Reverse Primer	TCT GGT TAC TGC CAG TTG AAT CTG	20uM
	2019-nCoV_N1-P	Probe	FAM-ACC CCG CAT TAC GTT TGG TGG ACC-BHQ1	10nmol
ORF1ab	SARS-CoV2.ORF1ab.F	Forward Primer	GGCCAATTCTGCTGTCAAATTA	20uM
	SARS-CoV2.ORF1ab.R	Reverse Primer	CAGTGCAAGCAGTTTGTGTAG	20uM
	SARS-CoV2.ORF1ab.P	Probe	FAM-ACAGATGTCTTGTGCTGCCGGTA-BHQ	10nmol

500

501

502

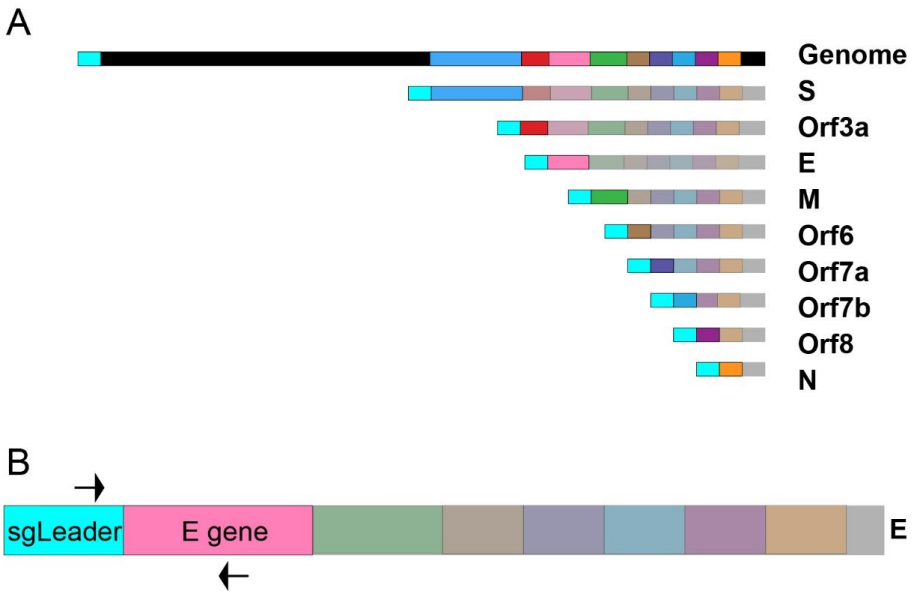

Figure 1

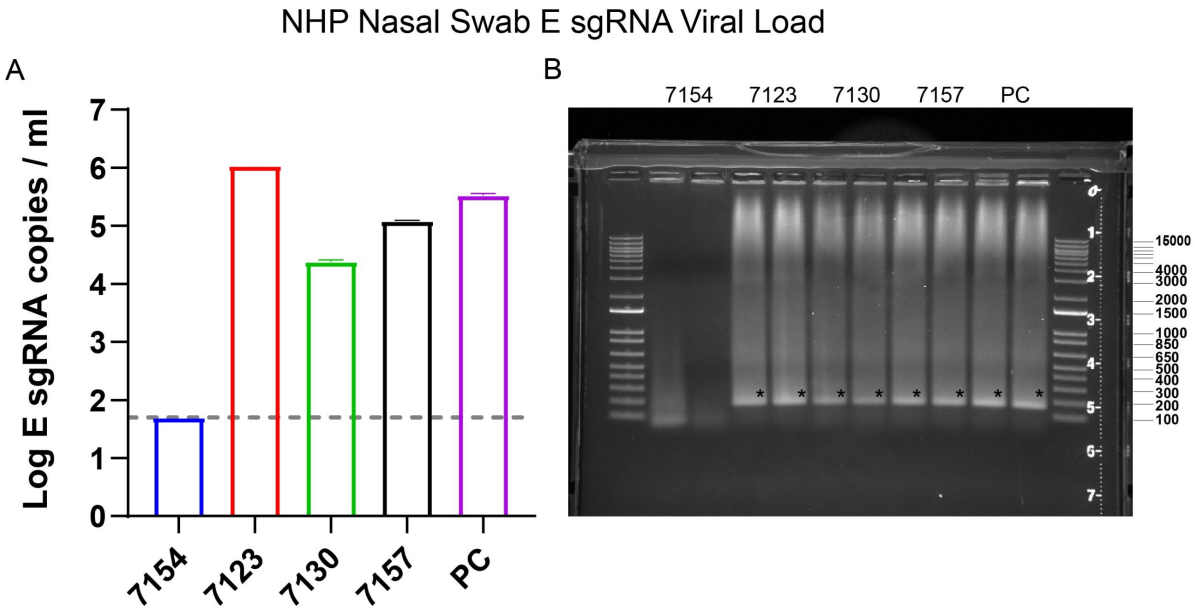

Figure 2

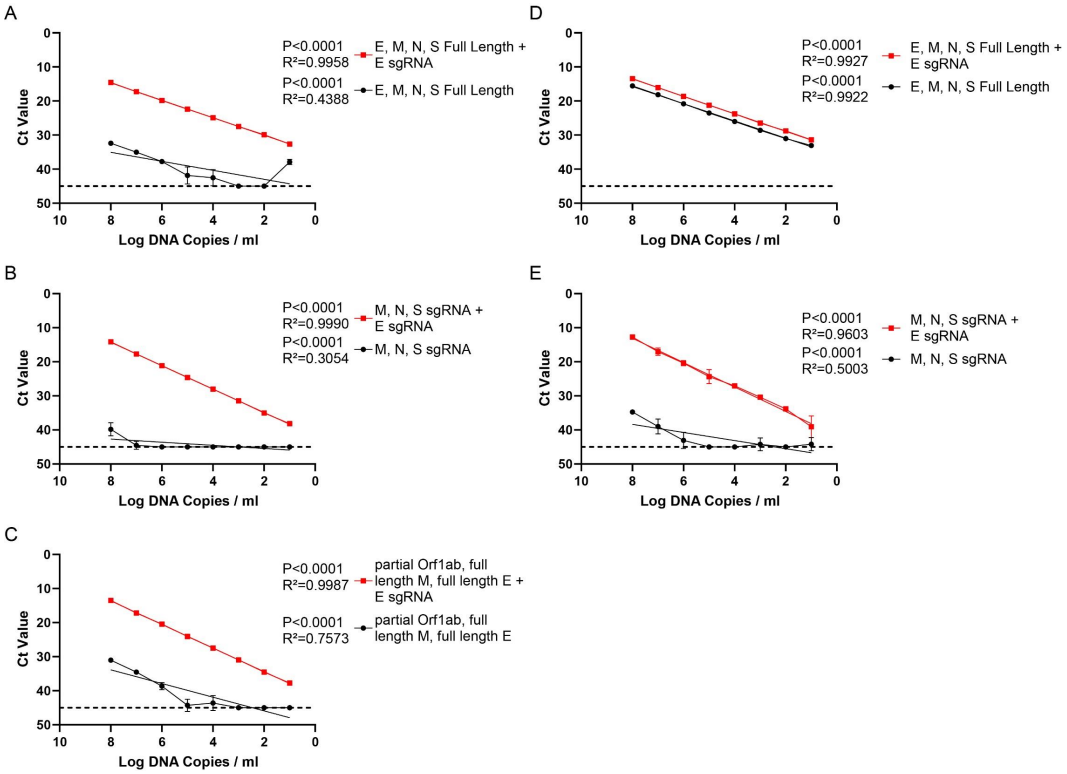

Figure 3

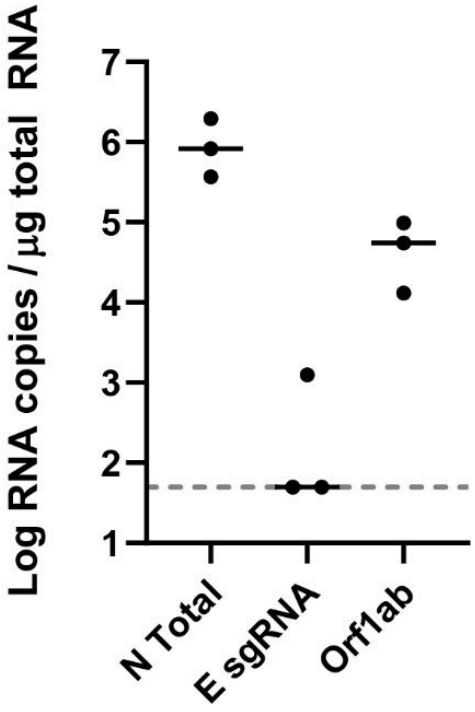

Figure 4

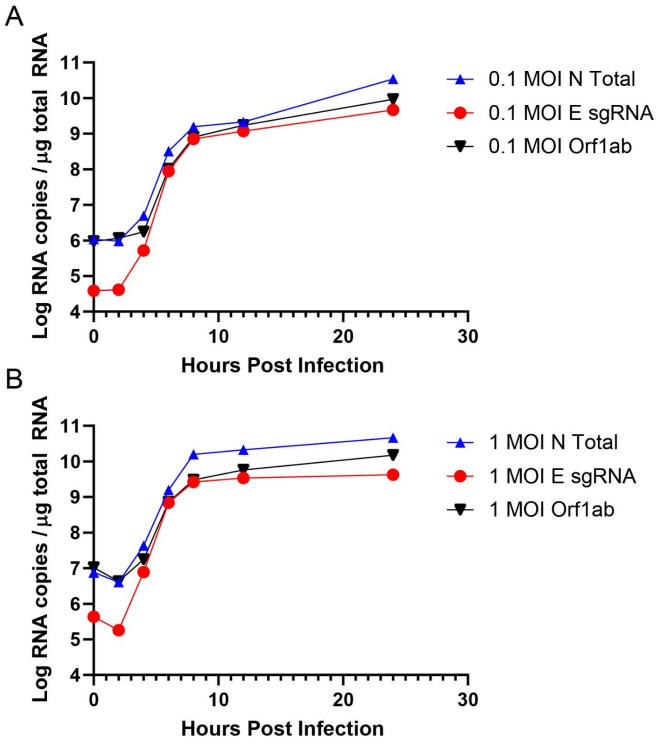

Figure 5

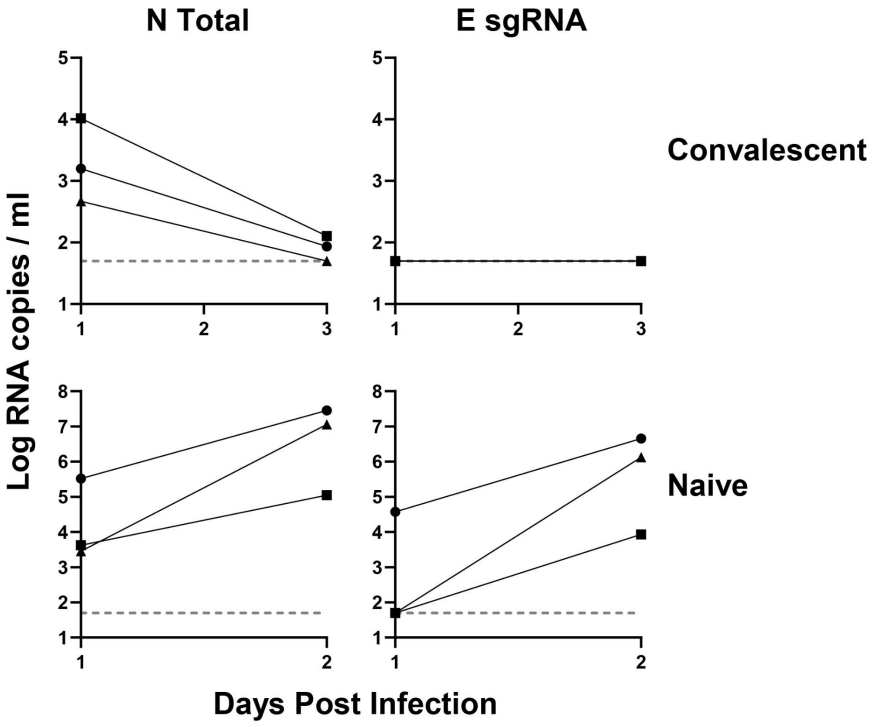

Figure 6

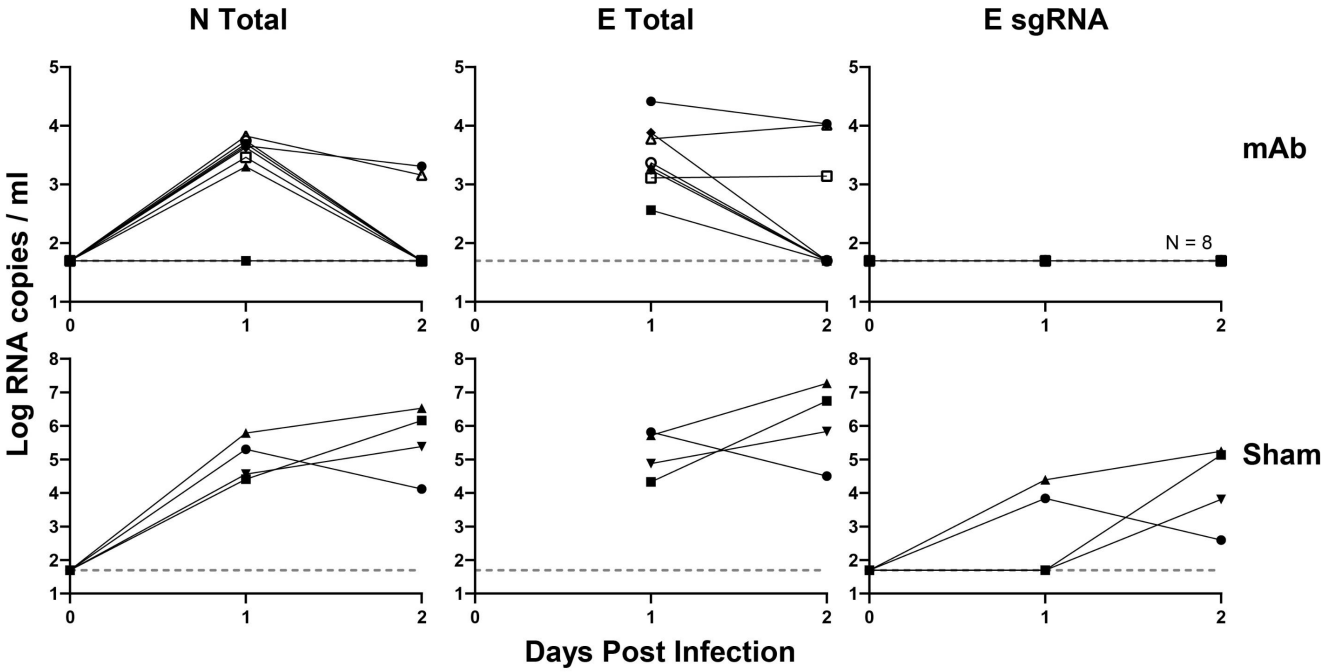

Figure 7